Conformational Studies by Dynamic NMR. 88.[1] Stereomutation Processes in the Diastereoisomers of a Representative Amino Alcohol and Related Amide Precursors†

Giuseppe Bartoli, Stefano Grilli, Lodovico Lunazzi, Massimo Massaccesi, Andrea Mazzanti,* and Samuele Rinaldi

Department of Organic Chemistry "A. Mangini", University of Bologna, Viale Risorgimento 4, Bologna 40136, Italy

mazzand@ms.fci.unibo.it

Received December 12, 2001

The barriers for three internal motions (i.e., phenyl and *tert*-butyl rotation as well as N-inversion) have been determined by dynamic NMR spectroscopy in the two diastereoisomeric forms of a typical amino alcohol [dimethylamino-2,4,4-trimethyl-3-phenyl-3-pentanol, $Me_2NCH_2CHMeC(OH)PhBu^t$]. The two structures were assigned by connection with those of the corresponding amide precursors determined by single-crystal X-ray diffraction. These amides (C═O in place of CH_2) too were found to undertake internal motions amenable to NMR observation, i.e., phenyl, *tert*-butyl, and N−CO rotations: the corresponding barriers were also measured. Ab initio computations indicate that H-bonding makes all these molecules adopt six-membered cyclic conformations, a conclusion which agrees well with the X-ray crystal structure determined for the amide precursors.

Introduction

Amino alcohols having the NR_2 and OH groups in a γ-relationship are an important class of compounds in organic chemistry, particularly because they can be employed as useful intermediates in the synthesis of many natural products, as is well documented in the recent literature.[2a] In addition, this structural unit, with a stereodefined geometry, is present in many relevant biological compounds.[2b] Likewise of great interest are their amide precursors (C═O in place of CH_2), since the N−CO bond represents the basic building block for many natural substances relevant to life processes. The stereodynamics occurring in amides are in fact involved in the interconversion pathways of the peptidyl bonds.[2c]

Surprisingly, quantitative experimental studies concerning the conformational changes occurring in amino alcohols have not been undertaken, to the best of our knowledge, despite the obvious interest commanded by this type of molecule.

In the present work we thus report a detailed investigation on the stereodynamics and on the conformational preferences of dimethylamino-2,4,4-trimethyl-3-phenyl-3-pentanol [$Me_2NCH_2CHMeC(OH)PhBu^t$] and of the corresponding amide precursor.

Chart 1. Schematic Representation of the Four Stereoisomers of $Me_2NCH_2CHMeC(OH)PhBu^t$

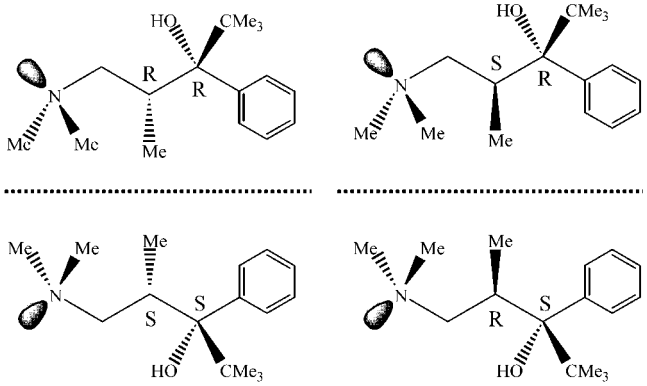

1 **2**

Results and Discussion

Both diastereoisomers (*R*,*R S*,*S* and *S*,*R R*,*S*) of the above-mentioned amino alcohols (**1** and **2** as in Chart 1) were separately obtained (see the Experimental Section).

The configurational assignment of **1** and **2** was obtained by relating these amines to the corresponding amide precursors, i.e., the diastereomeric forms (**3** and **4**) of 3-hydroxy-*N*,*N*,2,4,4-pentamethyl-3-phenylpentanamide [$Me_2NC(O)CHMeC(OH)PhBu^t$]. The assumption underlying this connection requires that the reduction of the NCO moiety of the amide group does not affect the configuration of the two stereogenic carbons.

X-ray diffraction (see the Experimental Section) shows that the two chiral carbons of amide **3** have opposite descriptors (i.e., *R*,*S* and *S*,*R*), so that for amine **1**,

* To whom correspondence should be addressed.

† Dedicated to Prof. Germana Mazzanti on the occasion of her retirement.

(1) Part 87: Anderson, J. E.; De Meijere, A.; Kozhushkov, S. I.; Lunazzi, L.; Mazzanti, A. *J. Am. Chem. Soc.*, in press. See also, Part 86: Dell'Erba, C.; Gasparrini, F.; Grilli, S.; Lunazzi, L.; Mazzanti, A.; Novi, M.; Pierini, M.; Tavani, C.; Villani, C. *J. Org. Chem.* **2002**, *67*, 1663.

(2) (a) Jäger, V.; Schwab, W.; Buss, V. *Angew. Chem., Int. Ed. Engl.* **1981**, *20*, 601. Ohfune, H. *Acc. Chem. Res.* **1992**, *25*, 360. Davies, S. G.; Ichihara, O. *Tetrahedron Lett.* **1999**, *40*, 9313. (b) Shibahara, S.; Kondo, S.; Maeda, K.; Umezawa, H.; Ohno, M. *J. Am. Chem. Soc.* **1972**, *94*, 4353. Kozikowski, A. P.; Chen, Y. Y. *J. Org. Chem.* **1981**, *46*, 5248. Hashiguchi, S.; Kawada, A.; Natsugari, H. *J. Chem. Soc., Perkin Trans. 1* **1991**, 2435. Knapp, S. *Chem. Rev.* **1995**, *95*, 1859. (c) Schreiber, S. L. *Science* **1991**, *251*, 238. Voet, D.; Voet, J. G. *Biochemistry*, 2nd ed.; Wiley: New York, 1995; p 200. Lu, K. P.; Hanes, S. D.; Hunter, T. A. *Nature* **1996**, *380*, 544. Hamilton, G. S.; Steiner, J. P. *J. Med Chem.* **1998**, *4*, 5119.

10.1021/jo016363e CCC: $22.00
Published on Web 03/23/2002

Chart 2. X-ray (Left) and Ab Initio Computed (Right) Structure of an Arbitrarily Selected Enantiomer of Amides 3 and 4[a]

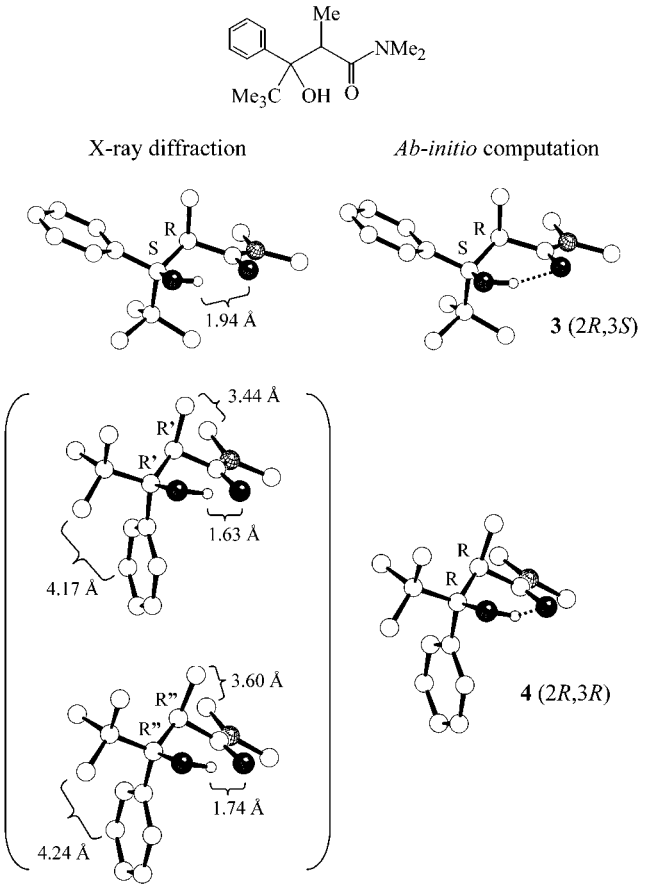

[a] In the case of **4** two independent structures were detected (see the text), and a few representative atomic distances (Å), outlining such a difference, are reported. The dotted line indicates the H-bonding between the OH and O═C moieties.

resulting from reduction of the NCO moiety of **3**, the *S,S* and *R,R* configurations were assigned, owing to the change in the priority of the substituents. The unit cell of racemic **3** comprises four molecules, i.e., two *R,S* and two *S,R* enantiomers: in Chart 2 one such enantiomer has been selected[3] for comparison with the corresponding ab initio computed[4] 2*R*,3*S* structure.

X-ray diffraction of racemic amide **4** indicates that the two chiral carbons have the same configuration (described as *R,R* or *S,S*), thus allowing us to assign, for the same reason, the pairs *S,R* and *R,S* to the related amine **2**. Eight molecules occupy the unit cell of **4**, with four of them (i.e., the two enantiomeric pairs *R′,R′* and *S′,S′*) having a distinct structure with respect to the other four (indicated as *R″,R″* and *S″,S″*). Two independent molecules, not related by any element of symmetry, were in fact observed, showing differences between the two sets of bond angles and bond lengths that by far exceed the experimental errors.

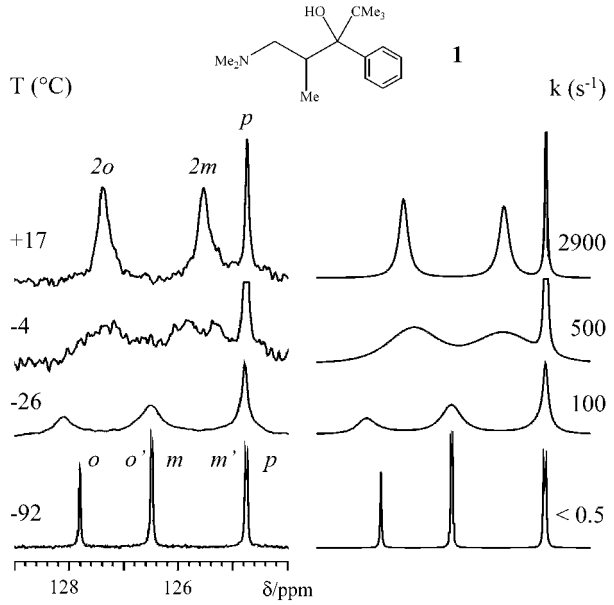

Figure 1. Experimental ^{13}C NMR (100.6 MHz in CD_2Cl_2) signals of the aromatic region of **1** as a function of temperature (left). The assignment of the *ortho* and *meta* ^{13}C lines was obtained by means of 2D correlations (gHSQC sequence) with the corresponding doublet and triplet ^1H signals. On the right is shown the computer simulation with the reported rate constants.

In Chart 2 (bottom) one enantiomer for each of the two different solid-state structures[3] is displayed: as long as they remain confined within the crystal,[5] these species should be considered two conformations of the same enantiomeric form. In Chart 2 is also reported the single *R,R* configuration computed[4] for the corresponding enantiomer of **4**: these calculations, in fact, cannot account for the two different structures created by the lattice interactions, since the theoretical approach refers to the case of an isolated molecule.

Inspection of the formulas of amines **1** and **2** suggests that three internal motions might be amenable to a quantitative determination by dynamic NMR spectroscopy, namely, rotation of the phenyl and *tert*-butyl groups as well as inversion at the nitrogen atom.

Variable-temperature ^{13}C NMR spectra of **1** (Figure 1, left) show indeed that the two single lines, corresponding to the pairs of *ortho* and *meta* carbons, broaden on cooling and eventually split into a pair of equally intense sharp lines since the carbons within each pair become diastereotopic, due to the negligible rotation rate about the Ph−C bond below −90 °C on the NMR time scale. The signal of the carbon in the *para* position, on the contrary, remains sharp because it lies on the rotation axis and therefore is not affected by this process. As a consequence five lines were observed at −92 °C for the five CH phenyl carbons, and line shape simulation (Figure 1, right) allowed the rate constants, hence the $\Delta G^{\ddagger}$ value (12.3 kcal mol^{-1} as in Table 1), to be determined for the rotation of the phenyl substituent.

In Figure 2 it is shown how the single ^{13}C line due to the three methyl carbons of the *tert*-butyl moiety of **1** broadens on lowering the temperature and displays three

(3) Of course the assignment of the 2*R*,3*S* rather than 2*S*,3*R* configuration to the enantiomer shown in the left-hand side picture of **3** (Chart 2) is arbitrary, as is the assignment of the *R,R* rather than the *S,S* configuration in the picture of **4**, since the absolute configuration cannot be deduced from X-ray diffraction lacking anomalous dispersion features.

(4) Ab initio calculations at the RHF 6.31G* level, Jaguar ver. 3.5.042.2 as implemented in the Titan 1,0,5 package, Wavefunction Inc., Irvine, CA.

(5) In solution and in the liquid state such a structural difference obviously disappears, and there is a unique structure which corresponds to the single enantiomeric form.

Table 1. Experimental Barriers (kcal mol^{-1}) for the Internal Motions of Derivatives 1−6[a]

	1	2	3	4	5	6
Ph rotation	12.3[c] at −4 °C (14.7)	11.9[c] at −15 °C (15.3)	15.8[b] at 70 °C	17.9[b] at 104 °C		
Bu^t rotation	10.0[c] at −59 °C (10.4)	9.4[c] at −70 °C (10.7)	6.3[c] at −140 °C	7.7[b] at −107 °C		
N-inversion	11.3[c] at −26 °C (12.6)	9.3[c] at −75 °C (11.7)			7.8[c] at −107 °C	7.5[c] at −111 °C
NCO rotation			19.7[b] at 118 °C	18.5[b] at 114 °C		

[a] In parentheses are shown the values computed[14] for amino alcohols **1** and **2**. [b] From ^{1}H spectra. [c] From ^{13}C spectra.

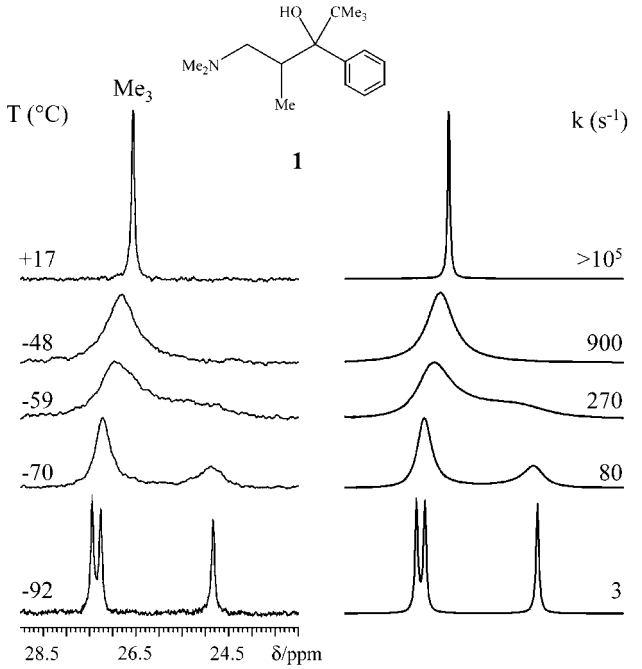

Figure 2. Experimental ^{13}C NMR (100.6 MHz in CD_2Cl_2) signals (left) of the *tert*-butyl methyl group of **1** as a function of temperature. On the right is shown the computer simulation with the reported rate constants.

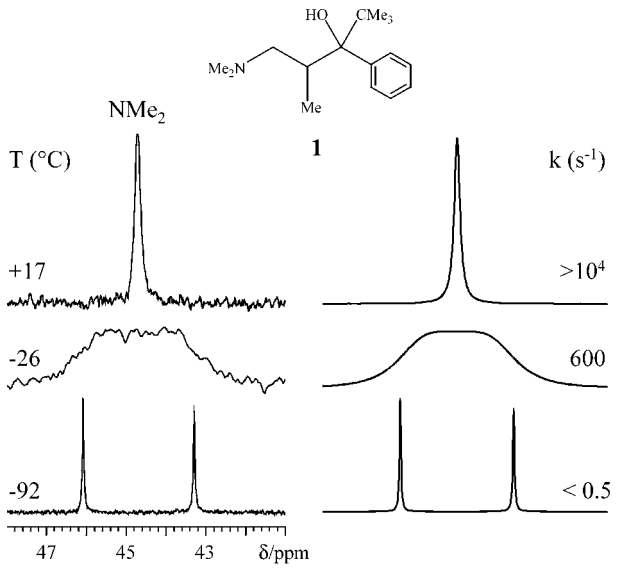

Figure 3. Experimental ^{13}C NMR (100.6 MHz in CD_2Cl_2) signals (left) of the *N*-methyl group of **1** as a function of temperature. On the right is shown the computer simulation with the reported rate constants.

equally intense lines at −92 °C: at this temperature the slow rotation about the C−Bu^t bond makes the three methyl groups diastereotopic, which consequently yield three anisochronous signals. The corresponding rotation barrier was found to be lower than that for phenyl ($\Delta G^{\ddagger}$ = 10.0 kcal mol^{-1}).

The third dynamic process observed involves the signal of two N-bonded methyl carbons: the corresponding ^{13}C line decoalesces below −26 °C (Figure 3), displaying two equally intense lines at −92 °C. Such a behavior can be understood by considering that when the rate of pyramidal inversion of nitrogen is slow on the NMR time scale, the two methyls are diastereotopic, since compounds **1** and **2** are chiral and thus devoid of a symmetry plane (which might otherwise make the *N*-methyl substituents enantiotopic). As a result, the *N*-methyl groups are anisochronous:[6,7] the NMe_2 group at low temperature (slow N-inversion) behaves like an isopropyl at any temperature in an asymmetric molecule.[8] Although usually referred to as N-inversion, this process should be more accurately described as a combination of N-inversion and C−N rotation.[7,9−11] The corresponding $\Delta G^{\ddagger}$ value was obtained by line shape simulation of the NMR traces and found equal to 11.3 kcal mol^{-1} (Table 1).

Analogous behavior was observed in the case of diastereomeric amine **2**, and for this reason these results are not described in detail: the corresponding $\Delta G^{\ddagger}$ values are collected in Table 1.

The N-inversion barrier of **2** (9.3 kcal mol^{-1}) is larger than that measured in analogous aliphatic dimethylamines such as Me_2NEt[6] and $Me_2NCHDBu^n$ [7] (their $\Delta G^{\ddagger}$ values are 8.6 and 8.2 kcal mol^{-1}, respectively): an even larger N-inversion barrier is that determined in the case of **1** (11.3 kcal mol^{-1}).

The occurrence of H-bonding is known to increase the N-inversion barrier of amines, as documented by the higher values observed when the measurements were carried out, for instance, in the presence of alcohol or water.[6,12] This is because the H-bonding to an essentially sp^3 hybridized lone pair lowers the energy of the pyramidal ground state relative to the sp^2 hybridized inversion transition state, where the lone pair is in a p-orbital which forms a weaker (if any) H-bond to the OH group. This effect is further increased in the case of intramolecular hydrogen bonds.[13]

(6) Casarini, D.; Davalli, S.; Lunazzi, L.; Macciantelli, D. *J. Org. Chem.* **1989**, *54*, 4616.
(7) Forsyth, D. A.; Johnson, S. M. *J. Am. Chem. Soc.* **1994**, *116*, 11481.
(8) Hanson, K. R. *J. Am. Chem. Soc.* **1966**, *88*, 2731. Mislow, K.; Raban, M. *Top. Stereochem.* **1967**, *1*, 1. Jennings, W. B. *Chem. Rev.* **1975**, *75*, 307. Eliel, E. L. *J. Chem. Educ.* **1980**, *57*, 52.
(9) Casarini, D.; Lunazzi, L.; Anderson, J. E. *J. Org. Chem.* **1993**, *58*, 714.
(10) (a) Bushweller, C. H. In *Acyclic Organonitrogen Stereodynamics*; Lambert, J. B., Takeuchi, Y., Eds.; VCH: New York, 1992; Chapter 1, p 1. (b) Brown, J. H.; Bushweller, C. H. *J. Phys. Chem.* **1994**, *98*, 11411. (c) Brown, J. H.; Bushweller, C. H. *J. Am. Chem. Soc.* **1995**, *117*, 12567 and references therein.
(11) Yamamoto, G.; Higuchi, H.; Yonebayashi, M.; Nabeta, I.; Ojima, J. *Tetrahedron* **1996**, *52*, 12409.
(12) Drakenberg, T.; Lehn, J. M. *J. Chem. Soc., Perkin Trans. 2* **1972**, 532.

Chart 3. Ab Initio Computed Structures of One Enantiomer Each of Amines 1 and 2[a]

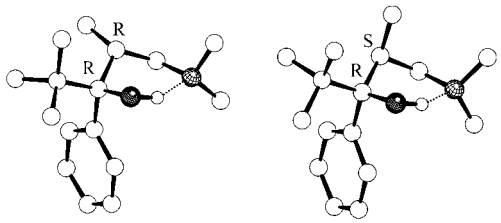

1 2

[a] The dotted line indicates the H-bonding between the OH and NMe_2 moieties.

Support of the existence of an intramolecular H-bond in **1** and **2** is offered by the significant low-field shift of their OH hydrogens. Moreover, the lower field shift observed in **1** (7.9 ppm) with respect to **2** (6.8 ppm) implies that the H-bond is stronger in **1**, thus accounting for the corresponding higher value of the N-inversion barrier.

By means of an appropriate computer program,[14] a search was made for all the possible conformations of **1** and **2**, and in both cases the most stable conformers were found to adopt a cyclic six-membered shape, where the relative positions of the OH and NMe_2 groups allow the existence of an intramolecular OH---N bond. The most stable conformers were subsequently investigated also by ab initio calculations[4] (Chart 3) that indicate how in both **1** and **2** the computed OH---N distance (1.85 Å) is well within the range expected for H-bonding. The second most stable conformer of **1** (according to ab initio calculations[4]) has a relative energy too high (ΔE = 2.24 kcal mol^{-1}) to be significantly populated. In the diastereoisomer **2**, on the contrary, the energy of the second most stable species is only 0.7 kcal mol^{-1} higher[4] and corresponds to an acyclic conformation where nitrogen and OH are too separated for displaying H-bonding (the OH---N computed[4] distance is 4.4 Å). The population of the latter, therefore, is not negligible, and an equilibrium between these two conformers would reduce the extent of the H-bonding and thus the N-inversion barrier (this hypothesis would also explain the trend of the OH shifts in **1** and **2**). The computed energy difference of 0.7 kcal mol^{-1} entails a proportion of the minor conformer of about 20% in the temperature range where the N-inversion barriers were measured, and indeed the barrier of **2** was found lower than that of **1**.

To obtain experimental support for the model described above, the intramolecular H-bonding was eliminated by substituting the OH group in **1** and **2** with an OMe group, thus obtaining the corresponding diastereoisomers of $Me_2NCH_2CHMeC(OMe)PhBu^t$ (**5** and **6**, respectively). According to MM calculations[14] neither of them is able to adopt the six-membered ring conformation brought about by H-bonding.

The measured N-inversion barriers (7.8 and 7.5 kcal mol^{-1}, respectively, for **5** and **6**) have essentially the same values, which are definitely lower than those of **1** and **2**. It is therefore unambiguously established that the presence of an intramolecular H-bond is responsible for the unusually high values observed for the N-inversion barrier in the amino alcohols **1** and **2**.

The *tert*-butyl and phenyl rotation barriers have almost equal values in **1** and **2**, indicating that in both diastereoisomers the environments hindering these motions are very similar. The rotation barrier for the *tert*-butyl is lower than that for the phenyl group, and this trend is matched by theoretical calculations.

MM computations[14] of the three-dimensional energy surface of **1** as a function of the C−Bu^t and C−Ph dihedral angles yields barriers of 10.4 and 14.7 kcal mol^{-1}, respectively, for the corresponding pathways displayed in Figure 4: analogous results were obtained from the surface computed for diastereoisomer **2** (Table 1). Although these calculations yield computed values exceeding those experimentally observed, they match the trend of the phenyl rotation barrier being higher than the *tert*-butyl rotation barrier.

Amides **3** and **4**, precursors of amines **1** and **2**, are also expected to display dynamic NMR features due to restricted rotation of the phenyl and *tert*-butyl groups: the measured values for the corresponding barriers are reported in Table 1. Nitrogen inversion, on the contrary, is NMR invisible in amides since the nitrogen atom has become essentially planar, due to the extent of conjugation with the carbonyl moiety (the sums of the three CNC angles determined by X-ray diffraction in **3** and **4** are, respectively, 359.9° and 359.8°, as expected for an essentially planar nitrogen atom). The N−CO double bond character is consequently quite high, making the corresponding rotation process[15] easily detectable by NMR spectroscopy. As shown in Figure 5, for instance, amide **4** displays two sharp ^1H lines for the *N*-methyl groups even at ambient temperature, and only above 115 °C do these lines coalesce into a single average signal. Line shape simulation yields a free energy of activation of 18.5 kcal mol^{-1}, and an even higher value (19.7 kcal mol^{-1}) was obtained in the case of the diastereomeric amide **3**. Both these values fall in the range typical for rotation processes in aliphatic amides.[16]

As shown in Chart 2 the experimental (X-ray) and computed structures indicate the existence of H-bonds between the CO and OH moieties in both amides **3** and **4** (the computed[4] CO---HO distances are, respectively, 1.86 and 1.75 Å, to be compared with the experimental distances of 1.94 Å in **3** and 1.73 and 1.64 Å for the two independent structures observed in the case of **4**). For this reason these amides adopt a six-membered cyclic structure: in the case of **3** the phenyl and *tert*-butyl groups occupy, respectively, the pseudoequatorial and pseudoaxial positions, whereas the reverse (see Chart 2) occurs in the case of **4** (the higher steric hindrance experienced by the phenyl in the pseudoaxial position in **4** makes the barrier for the corresponding 2-fold rotation process larger than that for the 2-fold rotation process involving the pseudoequatorial phenyl in **3**). Such a situation differs from that computed for the related amines, where the phenyl and *tert*-butyl groups adopt, respectively, the pseudoaxial and pseudoequatorial posi-

(13) Denisov, G. S.; Gindin, V. A.; Golubev, N. S.; Koltsov, A. I.; Smirnov, S. N.; Rospenk, M.; Koll, A.; Sobczyk, L. *Magn. Reson. Chem.* **1993**, *31*, 1034.

(14) MMFF force field ver. 6.0.6, as implemented in the computer package Titan 1,0,5, Wavefunction Inc., Irvine, CA.

(15) Pinto, M. In *Acyclic Organonitrogen Stereodynamics*; Lambert, J. B., Takeuchi, Y., Eds.; VCH: New York, 1992; Chapter 5, p 149.

(16) Oki, M. *Applications of Dynamic NMR Spectroscopy to Organic Chemistry*; VCH: Deerfield Beach, FL, 1986; p 44.

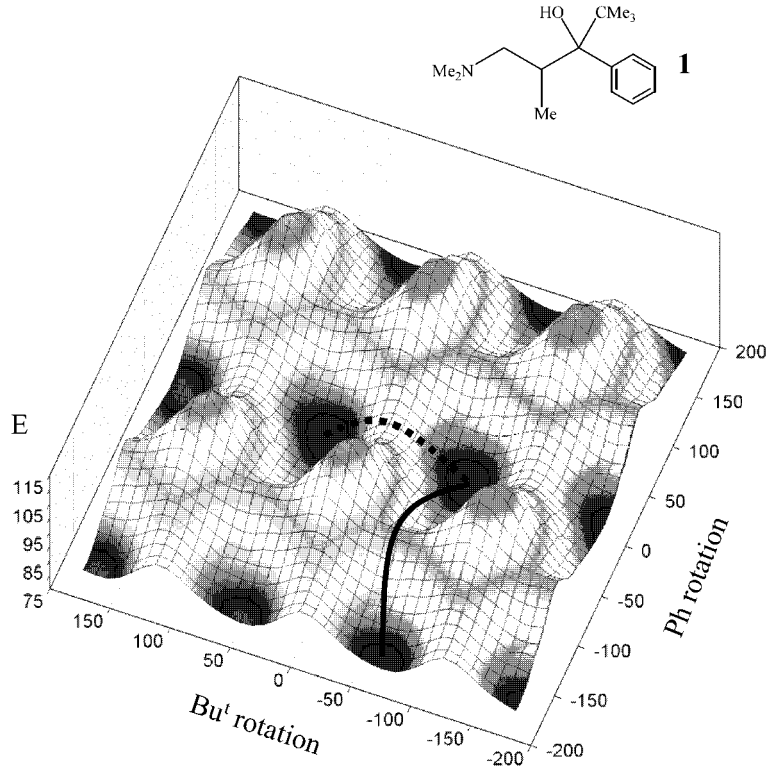

Figure 4. Energy (kcal mol^{-1}) surface computed[14] as a function of the torsion angles of the *tert*-butyl and phenyl groups in **1**. The full line represents the pathway for the phenyl rotation process (the dihedral angle being $C_2-C_1-C_q-O$) and the dotted line that for the *tert*-butyl rotation process (the dihedral angle being $Me-C_q-C_q-O$).

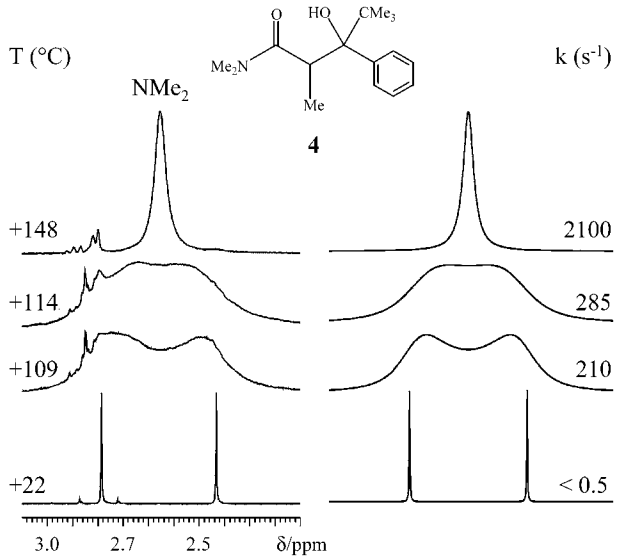

Figure 5. Experimental ^{1}H NMR (300 MHz in hexachloroacetone) signals of the *N*-methyl group of the amide moiety of **4** as a function of temperature (left). On the right is shown the computer simulation with the reported rate constants.

tions in both **1** and **2** (Chart 3).[17] The rotation barriers of the phenyl groups are larger, and those of the *tert*-butyl groups lower, in amides **3** and **4** with respect to the corresponding amino alcohols **1** and **2**: the steric hindrance experienced by the phenyl in amides, where nitrogen is essentially planar, is larger than that experienced in amines, where the nitrogen is pyramidal.[18] Also, the fact that amide **4** displays a lower N−CO rotation barrier (Table 1) than amide **3** depends on the stronger H-bond existing in the former with respect to the latter, as indicated by the shorter CO---HO distance observed in the crystal structure of **4**. It has been in fact observed[19] that the presence of H-bonding lowers the rotation barriers of amides.

Experimental Section

General Procedures. Flash chromatography was performed on Merck silica gel (0.040−0.063 nm) or Macherey−Nagel aluminum oxide, neutral. THF was dried by refluxing in the presence of sodium wire until the blue color of benzophenone ketyl persisted and then distilled into a dry receiver under nitrogen. ^{1}H and ^{13}C NMR spectra were recorded in $CDCl_3$. Coupling constants (*J*) are given in hertz. The ^{13}C NMR peak assignments are derived from DEPT experiments.

(2*R,3*S**)-3-Hydroxy-*N*,*N*,2,4,4-pentamethyl-3-phenylpentanamide (3)** was prepared by addition of *t*-BuMgCl−$CeCl_3$ complex to *N*,*N*,2-trimethyl-3-oxophenylpropanamide in the presence of $TiCl_4$, according to a recently reported[20] procedure (yield 60%, de > 98%). The spectral data agree with those of the literature.[20]

(17) In **1** and **2** the conformational assignment is based only on ab initio calculations in that the corresponding X-ray structures could not be obtained, these amino alcohols being liquid compounds. However, in view of the excellent agreement of this type of calculation with the X-ray structures of the corresponding amides **3** and **4**, such a theoretical assignment seems quite reliable.

(18) The opposite behavior observed for the *tert*-butyl groups in amines and amides might be explained by considering that the steric effect for the corresponding 3-fold rotation process is different, in principle, from that for the 2-fold rotation process involving the phenyl groups. Such a difference might even be so large as to reverse the trend of the corresponding barriers.

(19) Jackman, L. M.; Kavanagh, T. E.; Haddon, R. C. *Org. Magn. Reson.* **1969**, *1*, 109. Lewin, A. H.; Frucht, M. *Tetrahedron Lett.* **1970**, 1079. Hirota, M.; Todokoro, K. *Chem. Lett.* **1974**, 77. See also: Berg, U. *Acta Chem. Scand.* **1976**, *B30*, 695.

(20) Bartoli, G.; Bosco, M.; Marcantoni, E.; Massaccesi, M.; Rinaldi, S.; Sambri, L. *Tetrahedron Lett.* **2001**, *42*, 6093.

(2*R,3*R**)-3-Hydroxy-*N*,*N*,2,4,4-pentamethyl-3-phenylpentanamide (4)** was likewise prepared by addition of the $PhMgCl-CeCl_3$ complex to *N*,*N*,2,4,4-pentamethyl-3-oxopentanamide: yield 65%, de > 99%; ^1H NMR (200 MHz) δ 0.95 (s, 9H), 1.40 (d, $J_{HH} = 6.9$, 3H), 2.54 (s, 3H), 3.04 (s, 3 H), 3.69 (q, $J_{HH} = 6.9$, 1H), 6.03 (s, 1H), 7.00−7.40 (m, 4H), 7.75 (br d, 1H); ^{13}C NMR (75 MHz) δ 14.3 (CH_3), 27.6 (3 CH_3), 35.0 (C), 37.3 (CH_3), 38.6 (CH_3), 39.9 (CH), 80.3 (C), 124.6 (CH), 126.0 (CH), 126.1 (CH), 127.7 (CH), 127.9 (CH), 147.6 (C), 178.0 (C). Anal. Calcd for $C_{16}H_{25}NO_2$ (263.37): C, 72.97; H, 9.57. Found: C, 72.85; H, 9.50.

(2*R,3*R**)-(Dimethylamino)-2,4,4-trimethyl-3-phenyl-3-pentanol (1).** The appropriate hydroxy amide **3** (0.26 gr., 1 mmol), dissolved in 10 mL of THF, was reacted at ambient temperature with an excess of BH_3-THF complex for 48 h under an argon atmosphere. The solution was subsequently poured into aqueous HCl, treated with a 10% solution of NaOH until pH 10, and extracted with CH_2Cl_2. The organic layer was evaporated at reduced pressure and the residue dissolved in MeOH (6 mL) and then treated with 6 N HCl (2 mL). The reaction mixture was heated at 60 °C for 2 h and, after being cooled at ambient temperature, was evaporated under reduced pressure. The residue was subsequently dissolved in 5 mL of MeOH and evaporated again, repeating this operation three times. Finally the residue was diluted in water and treated with a 10% solution of NaOH until pH 10. The mixture was extracted with CH_2Cl_2, dried ($MgSO_4$), and concentrated under reduced pressure. The crude product was purified by chromatographic separation on a neutral aluminum oxide column (Et_2O/petroleum ether = 40/60): yield 70%, de > 99%; ^1H NMR (200 MHz) δ 0.95 (s, 9H), 1.13 (d, $J_{HH} = 7.4$, 3H), 1.72 (dd, $J_{HH} = 12.8$, $J_{HH} = 2.7$, 1H), 1.97 (s, 6H), 2.10 (d, $J_{HH} = 12.8$, 1H), 2.30−2.50 (m, 1H), 7.10−7.30 (m, 3H), 7.50 (br d, 2H), 7.90 (br s, 1H); ^{13}C NMR (50 MHz) δ 17.6 (CH_3), 27.0 (3 CH_3), 38.3 (CH), 39.5 (C), 45.0 (2 CH_3), 65.5 (CH_2), 82.9 (C), 125.9 (CH), 126.7 (CH), 128.4 (CH), 144.5 (C). Anal. Calcd for $C_{16}H_{27}NO$ (249.40): C, 77.06; H, 10.91. Found: C, 76.93; H, 10.85.

(2*R,3*S**)-(Dimethylamino)-2,4,4-trimethyl-3-phenyl-3-pentanol (2)** was obtained in the same way starting from amide **4**: ^1H NMR (200 MHz) δ 0.92 (s, 9H), 1.46 (d, $J_{HH} = 7.3$, 3H), 2.00 (br s, 7H), 2.30−2.50 (m, 2H), 7.10−7.35 (m, 3H), 6.80 (br s, 1H), 7.45−7.60 (m, 2H); ^{13}C NMR (75 MHz) δ 18.3 (CH_3), 27.7 (3 CH_3), 38.7 (C), 39.0 (CH), 47.4 (2 CH_3), 65.6 (CH_2), 82.9 (C), 125.7 (CH), 126.6 (CH), 127.2 (CH), 141.9 (C). Anal. Calcd for $C_{16}H_{27}NO$ (249.40): C, 77.06; H, 10.91. Found: C, 77.01; H, 10.88.

(2*R,3*R**)-3-Methoxy-*N*,*N*,2,4,4-pentamethyl-3-phenyl-1-pentanamine (5)** was prepared from the amino alcohol **1** according to a reported procedure,[21] with the following modifications. After the reaction was quenched with a saturated solution of NH_4Cl, a 10% solution of NaOH was added to the mixture until pH 10. The organic layer was extracted with CH_2Cl_2, dried over $MgSO_4$, and concentrated under reduced pressure. The crude product was purified by chromatographic separation on a neutral aluminum oxide column (Et_2O/petroleum ether = 10/90): ^1H NMR (300 MHz, CD_2Cl_2) δ 1.03 (s, 9H), 1.16 (d, $J_{HH} = 7.4$, 3H), 2.15 (dd, $J_{HH} = 12.5$, $J_{HH} = 6.0$, 1H), 2.38 (s, 6H), 2.75−2.85 (m, 1H), 3.35 (dd, $J_{HH} = 12.5$, $J_{HH} = 3.1$, 1H), 3.40 (s, 3H); ^{13}C NMR (75.5 MHz) δ 23.1 (CH_3), 28.8 (3 CH_3), 36.6 (CH), 41.0 (C), 46.6 (2 CH_3), 55.47 (CH_2), 65.0 (OMe), 89.3 (C), 127.3 (CH), 127.9 (CH), 131.3 (CH), 141.3 (C). Anal. Calcd for $C_{17}H_{29}NO$ (263.42): C, 77.51; H, 11.10. Found: C, 77.55; H, 11.04.

(2*R,3*S**)-3-Methoxy-*N*,*N*,2,4,4-pentamethyl-3-phenyl-1-pentanamine (6)** was prepared in the same way starting from the amino alcohol **2**: ^1H NMR (300 MHz) δ 1.00 (s, 9H), 1.50 (d, $J_{HH} = 6.7$, 3H), 2.23 (d, $J_{HH} = 12.5$, 1H), 2.30 (s, 6H), 2.43 (d, $J_{HH} = 12.5$, 1H), 2.75−2.88 (m, 1H), 3.34 (s, 3H); ^{13}C NMR (75.5 MHz) δ 18.5 (CH_3), 29.4 (3 CH_3), 37.9 (CH), 41.8 (C), 46.5 (2 CH_3), 55.1 (CH_2), 68.7 (OMe), 89.7 (C), 127.6 (CH), 128.4 (CH), 130.8 (CH), 143.1 (C). Anal. Calcd for $C_{17}H_{29}NO$ (263.42): C, 77.51; H, 11.10. Found: C, 77.55; H, 11.04.

X-ray Diffraction. Crystal Data of 3. $C_{16}H_{25}NO_2$ (263.37), monoclinic, space group $P2(1)_c$, $Z = 4$, $a = 9.6364(5)$ Å, $b = 13.2949(6)$ Å, $c = 12.4280(6)$ Å, $\beta = 103.660(10)°$, $V = 1547.14(13)$ Å^3, $D_c = 1.131$ g cm^{-3}, $F(000) = 576$, $\mu_{Mo} = 0.073$ mm^{-1}, $T = 293$ K. Data were collected using graphite-monochromated Mo Kα X-radiation ($\lambda = 0.71073$ Å), range $2.18° < \theta < 35.08°$. Of 27522 reflections collected, 6829 were found to be independent ($R_{int} = 0.0511$), 2116 of which were considered as observed [$I > 2\sigma(I)$], and were used in the refinement of 179 parameters, leading to a final R1 of 0.0466 and an R_{all} of 0.1538. The structure was solved by direct methods and refined by a full-matrix least-squares technique on F^2, using the SHELXTL 97 program packages. In the refinements weights were used according to the scheme $w = [\sigma^2(F_o^2) + (0.0838P)^2 + 0.0000P]^{-1}$, where $P = (F_o^2 + 2F_c^2)/3$. The hydrogen atoms were located by geometrical calculations and refined using a "riding" method, except for the OH hydrogen, which was experimentally located. wR2 was equal to 0.1353. The goodness of fit parameter *S* was 0.779. The largest differences between the peak and hole were 0.199 and −0.141 e Å^{-3}. Crystallographic data (excluding structure factors and including selected torsion angles) have been deposited with the Cambridge Crystallographic Data Center, CCDC Number 178970.

Crystal Data of 4. $C_{16}H_{25}NO_2$ (263.37), orthorhombic, space group $Pna2(1)$, $Z = 8$, $a = 11.3091(5)$ Å, $b = 17.2155(7)$ Å, $c = 16.4280(6)$ Å, $V = 3198.4(2)$ Å^3, $D_c = 1.094$ g cm^{-3}, $F(000) = 1152$, $\mu_{Mo} = 0.071$ mm^{-1}, $T = 293$ K. The unit cell contains two independent molecules; data were collected using graphite-monochromated Mo Kα X-radiation ($\lambda = 0.71073$ Å), range $1.71° < \theta < 30.00°$. Of 41197 reflections collected, 9300 were found to be independent ($R_{int} = 0.0466$), 4972 of which were considered as observed [$I > 2\sigma(I)$], and were used in the refinement of 351 parameters, leading to a final R1 of 0.0524 and an R_{all} of 0.1092. The structure was solved by direct methods and refined by a full-matrix least-squares technique on F^2, using the SHELXTL 97 program packages. In the refinements weights were used according to the scheme $w = [\sigma^2(F_o^2) + (0.0892P)^2 + 0.0000P]^{-1}$, where $P = (F_o^2 + 2F_c^2)/3$. The hydrogen atoms were located by geometrical calculations and refined using a "riding" method, except for the OH hydrogens, which were experimentally located. wR2 was equal to 0.1388. The goodness of fit parameter *S* was 0.954. The largest differences between the peak and hole were 0.151 and −0.143 e Å^{-3}. Crystallographic data (excluding structure factors and including selected torsion angles) have been deposited with the Cambridge Crystallographic Data Center, CCDC Number 178971.

NMR Measurements. The temperatures of the NMR probes were calibrated by substituting the samples with a precision Cu/Ni thermocouple before the measurements. Total line shape simulations were achieved by using a PC version of the DNMR-6 program.[22] The samples for the very-low-temperature measurements (range −100 to −140 °C) required for observing the *tert*-butyl rotation on amides **3** and **4** and N-inversion in **5** and **6** were prepared by connecting to the NMR tubes containing the desired compounds dissolved in C_6D_6 or CD_2Cl_2 to a vacuum line and condensing therein the gaseous CHF_2Cl solvent by means of liquid nitrogen. The tubes were subsequently sealed in vacuo and introduced into the precooled probe of the spectrometer.

Acknowledgment. Financial support has been received from MURST (national project "Stereoselection in Organic Synthesis") and from the University of Bologna (Funds for selected research topics 1999−2001).

JO016363E

(21) Casarini, D.; Lunazzi, L.; Mazzanti, A. *J. Org. Chem.* **1998**, *63*, 4746.

(22) QCPE program no. 633, Indiana University, Bloomington, IN.